

Measurement of nonresonant third-order susceptibilities of various gases by the nonlinear interferometric technique

Jae Won Hahn and Eun Seong Lee

*Division of Quantum Metrology, Korea Research Institute of Standards and Science,
P.O. Box 102 Yusong, Taejeon 305-600, Korea*

Received May 13, 1994; revised manuscript received November 14, 1994

We applied nonlinear interferometry of coherent anti-Stokes Raman spectroscopy (CARS) to measure the nonresonant third-order susceptibilities of various gases. Using argon as an internal calibration standard, we determined the effective nonresonant susceptibilities of acetylene, carbon dioxide, methane, nitrogen, oxygen, propane, carbon monoxide, Freon, and hydrogen from the amplitudes of the interference fringes of the CARS signals generated in the two gas cells. The electronic susceptibility was calculated by subtracting the off-resonant term of each molecule from the measured effective nonresonant susceptibility, and the results of this work are compared with the published data. The overall uncertainty is estimated to be less than 5%.

1. INTRODUCTION

Coherent anti-Stokes Raman spectroscopy (CARS) has been widely used as a diagnostic tool for probing temperature and species concentration of gas-phase samples.¹⁻⁶ CARS is considered one of the most useful noncontact diagnostic technique for studying combustion and gas flow in a hostile environment.⁷⁻¹⁰

The CARS signal is described by the square of the third-order nonlinear susceptibility $\chi_{\text{CARS}}^{(3)}$, which includes a resonant term χ_{R} and a nonresonant term χ_{NR} .^{11,12} For a gas mixture, χ_{R} indicates the resonant contribution from Raman transitions of the molecule under test and χ_{NR} indicates the sum of the off-resonant terms of the other molecules and the electronic contributions from all atoms and molecules in the gas mixture.

When the fractional concentration of a resonant molecule is of the order of a few percent, the nonresonant CARS term becomes comparable with the resonant term and produces modulation dips in the CARS spectrum.¹³ This deformation of the CARS spectrum by the nonresonant background makes curve fitting of the spectrum complicated, and the sensitivity of the concentration measurements is limited by the background. Temperature or species concentration measurements that use CARS, especially concentration measurements, are then only accurate to the degree to which the background nonresonant susceptibility is known.¹³⁻¹⁵ Several authors^{16,17} have proposed that concentration measurements be referenced to the magnitude of the nonresonant background. Therefore accurate values of the third-order nonresonant susceptibilities of various gases are important quantities in CARS thermometry.

Chang *et al.*¹⁸ first introduced the nonlinear interferometric technique to measure the relative phase between fundamental and second-harmonic light in a nonlinear optical material in 1965. Yacoby *et al.*¹⁹ applied this technique for cancellation of the nonresonant background in the CARS signal. They used a variable-length double cell that had three windows. The thick-

ness of the two cells was adjusted by movement of the two side windows. Recently Marowsky and Lupke²⁰ demonstrated a versatile experimental system for the control of the relative phase by spatially separating sample cells and placing a phase-shifting unit (PSU) between the sample cells. This system is more convenient for obtaining the interference fringes of the nonlinear signals as the pressure in the cell is constant during the entire experiment. We have adopted this technique to measure the nonresonant third-order susceptibilities of various gases.

The nonresonant susceptibilities of various gases have been measured by several nonlinear optical methods, such as wave mixing,²¹⁻²⁵ electric-field-induced second-harmonic generation,²⁶ and electro-optic Kerr effects.²⁷ In 1967 Rado²¹ first measured the third-order nonresonant susceptibility of several gases by using four-wave mixing based on the reference value of the resonant susceptibility of hydrogen. With the same technique, Lundeen *et al.*²² measured the nonresonant susceptibilities of a number of gases that included various hydrocarbons and halocarbons. Their reference value was the resonant susceptibility of hydrogen. Taking into consideration population factors and line widths, they reevaluated Rado's results. Using the Raman Q-branch resonance of deuterium as a reference, Rosasco and Hurst^{23,28} determined the absolute value of the nonresonant susceptibility of argon and hydrogen with phase-modulated coherent Raman spectroscopy. Finally, Farrow *et al.*^{14,25} obtained the nonresonant susceptibility of argon, nitrogen, and several other combustion gases by fitting the nitrogen-resonant CARS spectra for binary gas mixtures with the modified energy-gap model.

In this paper we propose a new technique for measuring the nonresonant susceptibility of gas: nonlinear interferometry. Using argon as a calibration standard, we obtain accurate values of the nonresonant susceptibilities of various gases relative to argon without any theoretical assumptions, and the results are compared with several previous determinations.

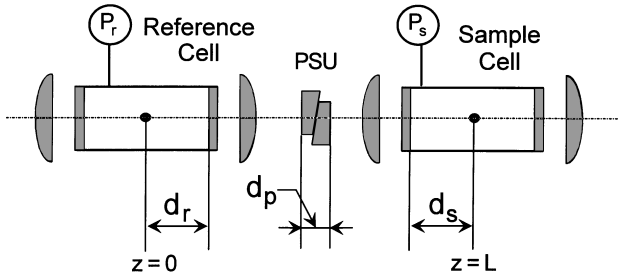


Fig. 1. Apparatus for nonlinear interferometry of CARS.

2. CALCULATION OF INTERFERENCE FRINGES OF THE CARS SIGNAL

Consider the apparatus shown in Fig. 1, which consists of two gas cells placed serially. One is the reference cell, which we fill with a reference gas (argon) that is to be used as an internal calibration standard, and the other is a sample cell, which we fill with the sample gas of interest. CARS signals are generated at $z = 0$ and $z = L$, and a PSU is placed between the cells to control the relative phase between the two CARS signals. The pump and Stokes beams for the CARS are collimated by a set of lenses and focused at $z = 0$ and $z = L$. Denoting the amplitude of the electric fields of the pump and the Stokes beams as E_{10} and E_{20} , respectively, the electric fields along the z direction in the reference cell are described by plane waves

$$E_{1r}(t, z) = E_{10} \exp[-i\omega_1 t + ik_r(\omega_1)z], \quad (1)$$

$$E_{2r}(t, z) = E_{20} \exp[-i\omega_2 t + ik_r(\omega_2)z], \quad (2)$$

where ω_1 and ω_2 are the frequencies of the pump and the Stokes beams, respectively, and k_r is the propagation vector in the reference gas.

Assuming that the CARS signal arises in the focal region by a short cylinder of length δ ($\ll 1$), we obtain for the CARS signal generated in the reference cell²⁹

$$E_{3r}(t, z) \cong ic_0 \delta \chi_r P_r E_{10}^2 E_{20}^* \exp[-i\omega_3 t + ik_r(\omega_3)z], \quad (3)$$

where $c_0 = 2\pi\omega_3/(n_{3r}c)$. Here χ_r and P_r are the CARS susceptibility and the pressure of the gas in the reference cell, respectively, n_{3r} is the refractive index of the gas, and c is the speed of light in vacuum.

Assuming that the depletion of the pump and the Stokes beams is negligible, we obtain the electric fields of the beams in the sample cell; the beams are propagated from the reference cell:

$$E_{1r}(t, z) = E_{10} \exp(-i\Delta_1) \exp[-i\omega_1 t + ik_s(\omega_1)z], \quad (4)$$

$$E_{2r}(t, z) = E_{20} \exp(-i\Delta_2) \exp[-i\omega_2 t + ik_s(\omega_2)z], \quad (5)$$

$$E_{3r}(t, z) \cong ic_0 \delta \chi_r P_r E_{10}^2 E_{20}^* \exp(-i\Delta_3) \times \exp[-i\omega_3 t + ik_s(\omega_3)z], \quad (6)$$

where Δ_i is the phase delay of the electric fields induced by propagation from the reference cell to the sample cell and is given by

$$\Delta_i = [k_s(\omega_i) - k_r(\omega_i)]d_r + [k_s(\omega_i) - k_p(\omega_i)]d_p + \gamma_i. \quad (7)$$

γ_i is the phase delay induced by air between the cells, the lenses, and the windows of the cells. k_s and k_p are

the propagation vectors in the sample cell and the PSU, respectively. The subscript i corresponds to 1, 2, and 3 for the pump beam, the Stokes beam, and the CARS signal, respectively.

At $z = L$, the electric field of the CARS signal becomes

$$E_{3r}(t, L) \cong ic_0 \delta \chi_r P_r E_{10}^2 E_{20}^* \exp(-i\omega_3 t) \exp\{i[k_r(\omega_3)d_r + k_p(\omega_3)d_p + k_s(\omega_3)d_s - \gamma_3]\}, \quad (8)$$

where d_r is the distance between the focal point in the reference cell and the right-hand window of the reference cell, as shown in Fig. 1, and d_s is the distance between the left-hand window of the sample cell and the focal point of the cell. d_p is the thickness of the PSU.

With the same assumptions that were used in deriving relation (3), we obtain the electric field of the CARS signal generated at $z = L$ in the sample cell:

$$E_{3s}(t, L) \cong ic_0' \delta \chi_s P_s E_{10}^2 E_{20}^* \exp(-i\omega_3 t) \exp\{i[2k_r(\omega_1)d_r + 2k_p(\omega_1)d_p + 2k_s(\omega_1)d_s - 2\gamma_1] - i[k_r(\omega_2)d_r + k_p(\omega_2)d_p + k_s(\omega_2)d_s - \gamma_2]\}, \quad (9)$$

where $c_0' = 2\pi\omega_3/(n_{3s}c)$. ϕ is a geometrical factor that represents the difference between the efficiency of the CARS signal generation in the reference cell and that in the sample cell. ϕ is affected by the aberration of the lenses and by scattering and absorption of the laser beam by the optical components. χ_s , P_s , and n_{3s} are the CARS susceptibility, the pressure, and the refractive index of the sample gas, respectively.

Assuming that the change of the refractive index is negligibly small, i.e., $c_0' = c_0$, we obtain for the intensity of the interference signal

$$I \propto |E_{3r} + E_{3s}|^2 \cong (c_0 \delta \chi_r P_r E_{10}^2 E_{20}^*)^2 \times [1 + \eta^2 + 2\eta \cos(\Delta k_r d_r + \Delta k_p d_p + \Delta k_s d_s - \Gamma)], \quad (10)$$

where

$$\eta = \frac{\chi_s P_s \phi}{\chi_r P_r},$$

$$\Gamma = 2\gamma_1 - \gamma_2 - \gamma_3,$$

$$\Delta k_j = 2k_j(\omega_1) - k_j(\omega_2) - k_j(\omega_3) \quad (j = r, s, p).$$

The subscript j corresponds to r , s , and p for the reference gas, the sample gas, and the PSU, respectively.

From relation (10) we find that the interference signal is modulated as a function of the phase delay induced by the dispersive media (gas cells, PSU, lenses, etc.), and a fringe pattern arises. We note that if we fix the pressure of the reference cell, the amplitude of the interference fringes, η , linearly depends on the pressure of the sample cell.

A. Change of Thickness of the PSU

If we change the thickness of the PSU, the intensity of the interference signal in relation (10) becomes

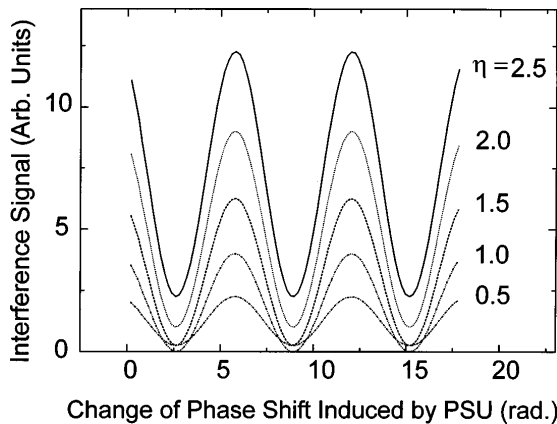


Fig. 2. Intensity of the interference signal calculated by changing the phase shift induced by the PSU at several η in relation (10).

$$I \cong (c_0 \delta \chi_r P_r E_{10}^2 E_{20}^*)^2 [1 + \eta^2 + 2\eta \cos(\Delta k_p d_p + \Gamma')], \quad (11)$$

where $\Gamma' = \Delta k_r d_r + \Delta k_s d_s - \Gamma$. Figure 2 shows the calculated fringe patterns of the interference signal. For the calculation we assume $\phi = 1$, and the calculation of the interference fringe is performed as a function of the phase shift $[\Delta k_p d_p$ in relation (11)] induced by the PSU.

B. Change of Pressure of the Sample Cell

If we assume that the refractive index of the gas sample depends linearly on the gas pressure, the refractive index n_s is given by³⁰

$$n_s \cong 1 + \alpha P \quad (\alpha \ll 1). \quad (12)$$

Then we find the intensity of the interference signal to be

$$I \cong (c_0 \delta \chi_r P_r E_{10}^2 E_{20}^*)^2 \times [1 + \xi^2 P_s^2 + 2\xi P_s \cos(2\pi \Delta \alpha P_s d_s + \Gamma'')], \quad (13)$$

where

$$\xi = \frac{\chi_s \phi}{\chi_r P_r},$$

$$\Delta \alpha = \frac{2\alpha(\omega_1)}{\lambda_1} - \frac{\alpha(\omega_2)}{\lambda_2} - \frac{\alpha(\omega_3)}{\lambda_3},$$

$$\Gamma'' = \Delta k_r d_r + \Delta k_p d_p + \Delta k_s d_s - \Gamma,$$

$$\Delta k_0 = \frac{1}{c}(2\omega_1 - \omega_2 - \omega_3).$$

Figure 3 shows the calculated interference signal as a function of the pressure of the sample cell. For the calculation ϕ , $\Delta \alpha$, and d_s in relation (13) are given by 1, $1.56 \times 10^{-5} \text{ (bar cm)}^{-2}$ (1 bar = 749.9 Torr), and 8 cm, respectively. We find that it is hard to derive any physical parameter—the magnitude of the susceptibility, for example—by fitting the interference fringe in Fig. 3.

3. EXPERIMENT

The detailed description of the CARS spectrometer used in this investigation was given previously,³¹ and only a brief description will be given here. A simple schematic diagram for the nonlinear interferometry of CARS is shown in Fig. 1. A frequency-doubled Nd:YAG laser (Quantel

YG660-10) produced 532-nm light of $\sim 150\text{-mJ/pulse}$ energy, 7–8-ns pulse duration, at a 10-Hz repetition rate. Some of the energy of the doubled Nd:YAG laser ($\sim 90\%$) was used to pump a pulsed dye laser (Lumonics Hyper Dye SLM), and the remaining beam was used for the two pump beams for boxcars phase matching³² of the CARS experiment.

We operated the Nd:YAG laser in a single longitudinal mode by injection locking with a diode-pumped cw Nd:YAG laser (Light Wave S-100), and the spectral bandwidth of the laser pulse was less than 100 MHz.³³ The pulsed dye laser was operated in a single longitudinal mode by the grazing-incidence beam technique,³⁴ and the bandwidth of the laser pulse was ~ 500 MHz. The stability of the single-mode operation of the pulsed dye laser in scanning the frequency was not confirmed, but, after careful alignment of the laser, we found that the stability of the single-mode operation was good enough for this investigation when we held the frequency of the pulsed dye laser at a constant value.

For the boxcars phase matching the distance between the axes of the two pump beams was 5–6 mm and the waists of the pump and the Stokes beams in the collimating lens were ~ 2 mm. Spatial resolution, which was measured by purging dried argon through a slit-type nozzle, was 2–3 mm. The pump and the Stokes beams were collimated with a set of achromatic lenses ($f = 25$ cm) to maintain the symmetry of the beam configuration. The pump and the Stokes beams were horizontally polarized, and we recorded the CARS signal with the same polarization.

Using the nonresonant CARS signal arising in another gas cell (propane ~ 2 bars) that was installed behind the sample cell, we normalized the CARS signals on a shot-by-shot basis for the laser intensity fluctuations. This reduced the peak-to-peak noise of the CARS signal by a factor of 8. We measured the CARS signal with a photomultiplier tube (PMT) (EMI 9658) after the signal passed through a monochromator (Jobin Yvon U-1000), and we used another set of a PMT (Hamamatsu R955) and a monochromator (Jobin Yvon HR-320) for detecting the nonresonant CARS signal. The PMT signals were received by a two-channel boxcar averager (Stanford Research SR-250), and the data were recorded by a computer (IBM 386 compatible) interfaced with the boxcar

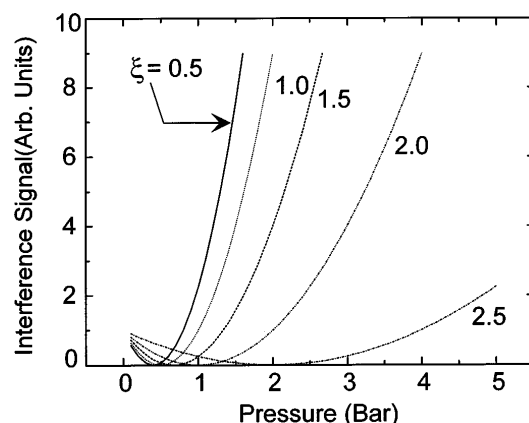


Fig. 3. Intensity of the interference signal calculated by changing the pressure of the sample cell at several ξ in relation (13).

averager. The PSU consisted of a pair of wedges made of BK-7 glass, and we automatically changed its thickness by sliding a wedge with a stepping motor interfaced with the computer.

In this experiment accurate measurement of the pressure is important. Before each measurement we evacuated the whole gas line, including gas cells, at a pressure of less than 100 mTorr and flushed it with the filling gas. The pressure of the reference and the sample gases was measured with a pressure transducer (Druck PDCR-911). We applied the bias voltage of the transducer with a precision power supply (HP 6115A) and read the voltage signal with a $5^{1/2}$ -digit digital voltmeter (HP 3478A). We calibrated the transducer (with the power supply and the voltmeter) as a system against a piston gauge (Ruska 2465) for 20 points in pressure ranging up to 2 bars. The estimated uncertainty of the calibration was less than 0.1% of the reading value.

Using argon (Matheson 99.9995%) as an internal calibration standard, we measured the relative magnitude of the nonresonant third-order susceptibility of various gases: acetylene (C_2H_2 , 99.6%), carbon dioxide (CO_2 , 99.99%), methane (CH_4 , 99.8%), nitrogen (N_2 , 99.99%), oxygen (O_2 , 99.99%), propane (C_3H_8 , 99.5%), carbon monoxide (CO , 99.95%), Freon (CF_4 , 99.7%), and hydrogen (H_2 , 99.999%). Most of the sample gases were supplied by Korean Special Gas Company, except argon and Freon (Matheson, Freon-14).

Defining the contrast of the interference fringes as the ratio of the maximum to the minimum of the interference signals, we obtained the highest contrast when filling the reference and the sample cells with the same gas at the same pressure. The contrast strongly depends on the alignment of the entire system, the bandwidth of the laser pulses, the window contamination, etc. The nominal highest contrast during the experiment was above 100. The measurements were performed at the Raman shift, 2157 or 2334 cm^{-1} , to avoid the Raman resonance line of nitrogen or carbon monoxide, respectively.

4. RESULTS AND ANALYSIS

Filling both the reference and the sample cells with argon at the pressure of 0.99 bar and 0.51 bar, respectively, we obtained a typical interference fringe by changing the thickness of the PSU; the fringe pattern is shown in Fig. 4. The coherence length¹⁸⁻²⁰ given in the figure is $2\pi/\Delta k_p$. Each data point denoted by a cross (+) is the average of 5 shots that were normalized for the laser intensity fluctuation. The solid line is the result of least-squares curve fitting with relation (11), and we determined the amplitude of the fringes for a given pressure of the sample cell.

To obtain the ratio of the nonresonant susceptibility of the various gases to that of argon, we first filled both the reference and the sample cells with argon and measured the amplitude of the interference fringe by changing the thickness of the PSU at several pressures of argon in the sample cell. The results are shown in Fig. 5. The straight line in Fig. 5 is the result of a linear regression of the data points. We found that the data points are nicely fitted by the straight line with a very small intercept.

After evacuating the sample cell and then filling the cell with the sample gas being tested, we measured the amplitudes of the interference fringes at several pressures of the sample gas. The amplitudes of the fringe for the sample gases were normalized with the amplitudes of the fringe of argon at each corresponding pressure, and the results are plotted in Fig. 6. The straight lines in Fig. 6 are the results of linear regressions to the data points of each sample gas. We note that the intercepts of all the straight lines shown in Fig. 6 are negligibly small. From the fitting procedure, we extracted the ratios of the slope of the interference fringe of the various gases to that of argon, which gives us the value of the effective third-order susceptibilities of the sample gases relative to that of argon.

The ratio of the slopes and the calculated effective susceptibilities of the various gases are listed in Table 1. For the calculation of the effective susceptibility, the value of the nonresonant susceptibility of argon reported by Rosasco and Hurst²³ was used. The values in the parentheses are the estimated uncertainties in the determined values. We evaluated the uncertainties by accounting for the uncertainties in determining the slopes of the interference fringes of argon and the sample gas, the intercepts of the linear regressions, and the pressure measurement. The uncertainty of the ratio of the slope for most of the

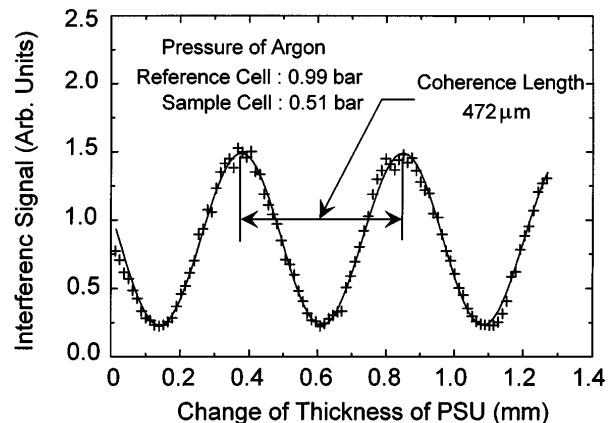


Fig. 4. Typical interference fringe obtained by filling both the reference and the sample cells with argon at the pressure listed.

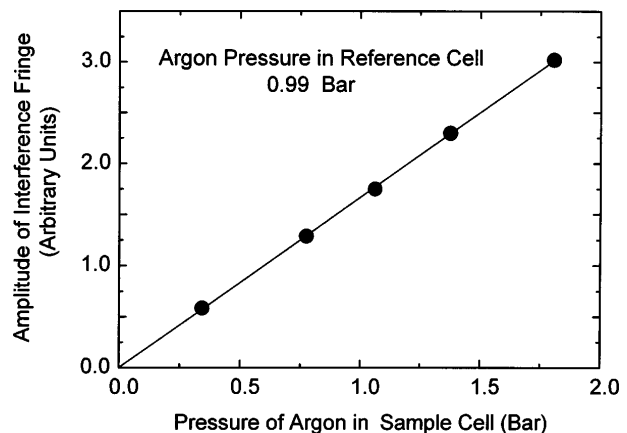


Fig. 5. Amplitude of the interference fringe measured by changing the thickness of the PSU at several pressures of argon in the sample cell.

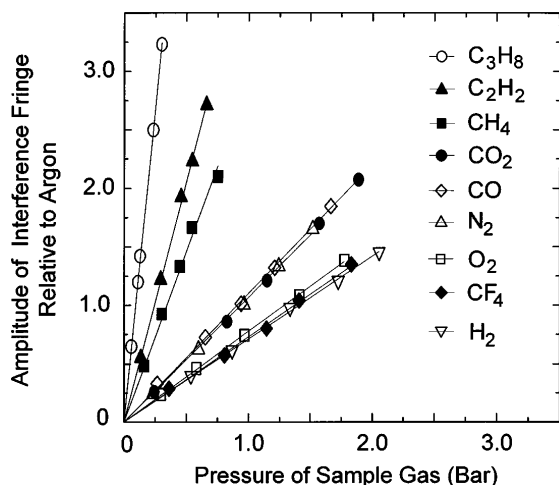


Fig. 6. Amplitudes of the interference fringes measured by changing the thickness of the PSU at several pressures of the sample gases in the sample cell. The amplitudes of the fringe for the sample gases were normalized with the amplitudes of the fringe of argon at each corresponding pressure.

gases in Table 1 is usually about 2–3% and is no larger than 5%.

To determine the pure electronic nonresonant susceptibility of the gases, we have to subtract the off-resonant Raman susceptibility from the effective nonresonant susceptibility. The CARS susceptibility is generally given

by the following expression¹¹:

$$\chi_{\text{CARS}}^{(3)} = \frac{N}{\hbar} \sum_{a,b} (\rho_{aa} - \rho_{bb}) \frac{c^4}{\omega_1 \omega_2^3} \frac{d\sigma}{d\Omega} \times \frac{1}{\omega_{ba} - \omega_1 + \omega_2 + i\gamma_{ba}}, \quad (14)$$

where N is the total number of molecules per unit volume, ρ_{aa} and ρ_{bb} are the population in the ground state and the upper state of the Raman transition line, respectively, $d\sigma/d\Omega$ is the Raman cross section, ω_{ba} is the Raman transition frequency, and γ_{ba} is the linewidth of the Raman transition due to the relaxation processes. In the off-resonant region, $|\omega_{ba} - \omega_1 + \omega_2| \ll \gamma_{ba}$, and we can neglect $i\gamma_{ba}$. Then we get

$$(\chi_{\text{CARS}}^{(3)})_{\text{off}} = \frac{N}{\hbar} \sum_{a,b} (\rho_{aa} - \rho_{bb}) \frac{c^4}{\omega_1 \omega_2^3} \frac{d\sigma}{d\Omega} \frac{1}{\omega_{ba} - \omega} \quad (15)$$

for the off-resonant Raman susceptibility, where ω is the Raman shift ($= \omega_1 - \omega_2$). The off-resonant Raman susceptibility in relation (15) comes mainly from the vibrational-rotational Q branch of each molecule. The magnitudes of the Raman cross section^{34,35} are listed in Table 2, and the references of the molecular constants used for determining the Raman transition line of the molecule are listed in the same table. Using relation (15) and the Raman cross section listed in Table 2, we calculated the off-resonant term; the calculated off-resonant

Table 1. Determined Effective Susceptibility $\chi_{\text{NR}}^{(3)}$

Gas	Ratio ^a	Effective $\chi_{\text{NR}}^{(3) b}$ [$10^{-18} \text{ cm}^3/(\text{erg amagat})$]	Raman Shift (cm^{-1})
Acetylene	4.11 (0.08)	38.9 (0.76)	2157
Carbon dioxide	1.14 (0.05)	10.8 (0.5)	2157
Methane	2.84 (0.15)	26.9 (1.4)	2157
Nitrogen	1.08 (0.02)	10.2 (0.2)	2157
Oxygen	0.773 (0.019)	7.31 (0.18)	2157
Propane	10.7 (0.39)	101.2 (3.7)	2157
Carbon monoxide	1.09 (0.03)	10.3 (0.3)	2334
Freon	0.730 (0.026)	6.91 (0.25)	2334
Hydrogen	0.704 (0.018)	6.66 (0.17)	2334

^aRatio of the slope of the interference fringe of the sample gas to that of argon (estimated uncertainties are shown in parentheses).

^bThe effective susceptibility $\chi_{\text{NR}}^{(3)}$ is calculated based on the value of the nonresonant susceptibility of argon ($9.46 \times 10^{-18} \text{ cm}^3/\text{erg amagat}$) reported by Rosasco and Hurst.²³

Table 2. Raman Cross Section and the Calculated Off-resonant Term

Gas	Raman Band (cm^{-1})	Raman Cross Section ^a ($10^{-31} \text{ cm}^2/\text{sr}$)	References for Molecular Constants	Off-resonant Term [$10^{-18} \text{ cm}^3/(\text{erg amagat})$]	
				at 2157 cm^{-1}	at 2334 cm^{-1}
Acetylene	1973	23.76	37	-12.00	—
Carbon dioxide	1285	3.37	38	-0.35	—
Carbon dioxide	1388	5.23	38	-0.62	—
Methane	2917	39.31	39	4.17	—
Nitrogen	2331	4.32	37	2.30	—
Oxygen	1555	4.41	40	-0.67	—
Propane	2890	100.0	41	12.5	—
Carbon monoxide	2143	4.15	37	—	-2.03
Freon	1283	3.01	40	—	-0.24
Hydrogen	4156	14.9	37	—	0.77

^aRefs. 34 and 35.

Table 3. Electronic Susceptibilities $\chi_{NR}^{(3)}$ of Various Gases (10^{-18} cm³/(erg amagat)^a

Gas	This Experiment	IRS ^b 676 + 584 nm	CARS ^c 532 + 607 nm	EHSG ^d 694 nm	CARS ^e 532 + 683 nm	CARS ^f 532 + 683 nm	CARS ^g 694 + 976 nm
Argon	(9.46)	9.46	9.6	9.2	–	10.56	9.31
Acetylene	50.9						
Carbon dioxide	11.8			10.6	9.1	12.3	12.02
Methane	22.7			25.6	31.3	26.6	17.72
Nitrogen	7.90		8.5	7.2	7.0	8.47	8.11
Oxygen	7.98			7.6	7.7	11.4	7.81
Propane	88.7		80	84.6			
Carbon monoxide	12.3			13.6		12.5	11.81
Freon	7.15			8.9			
Hydrogen	5.90	5.34		5.4	6.9		

^aThe uncertainties of the absolute values of the electronic susceptibility $\chi_{NR}^{(3)}$ listed in this table are estimated to be 10%.

^bIRS, inverse Raman spectroscopy, Refs. 23 and 28.

^cRefs. 15 and 25.

^dEHSG, static electric-field-induced second-harmonic generation, Ref. 42.

^eEffective $\chi_{NR}^{(3)}$ obtained by comparing the absolute intensities of the nonresonant CARS signals of two gases in a USED CARS configuration.

^fCARS, Ref. 22.

^gCARS, Ref. 21, reevaluated data; see text.

terms of the sample gases used in this investigation are given in Table 2 also.

The electronic susceptibility $\chi_{NR}^{(3)}$ of the various gases determined in this investigation are summarized in Table 3 and compared with several previous determinations. The results of Rado²¹ are the reevaluated data that were calculated reflecting the more accurate value of the susceptibility for the hydrogen Q(1) line reported by Rosasco and Hurst.²³ Most values of the electronic susceptibilities reported here are in reasonable agreement with the literature data listed in Table 3. To confirm the measurement technique, we measured the effective susceptibility of oxygen again at a different Raman shift of 2334 cm⁻¹, and we obtained the value of $7.28 \times 10^{-18} \pm 0.18$ cm³/(erg amagat). When we subtracted the off-resonant term of oxygen, -0.53×10^{-18} cm³/(erg amagat) at the Raman shift, we found the electronic susceptibility of oxygen to be 7.81×10^{-18} cm³/(erg amagat) at 2334 cm⁻¹, which differs by only 2.1% from the value listed in Table 3 measured at 2157 cm⁻¹.

5. CONCLUSIONS

We have demonstrated the application of the nonlinear interferometric technique to the measurement of the nonresonant third-order susceptibilities of various gases. With this technique we reduce measurement errors by direct comparison of the nonresonant signal of a reference with that of a sample gas and by linear regression of the data obtained at several pressures. This technique is especially useful for measuring the nonresonant third-order susceptibility of gaseous samples whose nonlinear optical signals are weak. We estimate that overall uncertainty associated with this technique is less than 5%.

ACKNOWLEDGMENTS

We thank J. P. Looney at the National Institute of Standards and Technology for helpful discussions. This re-

search was supported by the Korean Ministry of Science and Technology.

REFERENCES

1. P. R. Regnier and J. P. E. Taran, "On the possibility of measuring gas concentrations by stimulated anti-Stokes scattering," *Appl. Phys. Lett.* **23**, 240–242 (1973).
2. W. B. Rho, P. W. Schreiber, and J. P. E. Taran, "Single-pulse coherent anti-Stokes Raman scattering," *Appl. Phys. Lett.* **29**, 174–176 (1976).
3. I. A. Stenhouse, D. R. Williams, J. B. Cole, and M. D. Swords, "CARS measurements in an internal combustion engine," *Appl. Opt.* **18**, 3819–3825 (1979).
4. W. M. Tolles, J. W. Nibler, J. R. McDonald, and A. B. Harvey, "A review of the theory and application of coherent anti-Stokes Raman spectroscopy," *Appl. Spectrosc.* **31**, 253–271 (1977).
5. L. A. Rahn, S. C. Johnston, R. L. Farrow, and P. L. Mattern, "CARS thermometry in an internal combustion engine," in *Temperature, Its Measurement and Control in Science and Industry*, J. F. Schooley, ed. (Instrument Society of America, Pittsburgh, 1982), Vol. 5, Part 1, pp. 609–613.
6. A. C. Eckbreth, G. M. Dobbs, J. H. Stufflebeam, and P. A. Tellex, "CARS temperature and species measurements in augmented jet engine exhausts," *Appl. Opt.* **23**, 1328–1339 (1984).
7. G. L. Switzer, W. M. Roquemore, R. B. Bradley, P. W. Schreiber, and W. B. Rho, "CARS measurements in a bluff-body stabilized diffusion flame," *Appl. Opt.* **18**, 2343–2345 (1979).
8. D. A. Greenhalgh, F. M. Porter, and W. A. England, "The application of coherent anti-Stokes Raman scattering to turbulent combustion thermometry," *Combust. Flame* **49**, 171–181 (1983).
9. W. A. England, J. M. Milne, S. N. Jenny, and D. A. Greenhalgh, "Application of CARS to an operating chemical reactor," *Appl. Spectrosc.* **38**, 867–875 (1984).
10. D. A. Klick, K. A. Marko, and L. Rimai, "Broadband single-pulse CARS spectra in a fired internal combustion engine," *Appl. Opt.* **20**, 1178–1181 (1981).
11. S. A. J. Druet and J. P. E. Taran, "CARS spectroscopy," *Prog. Quantum Electron.* **7**, 1–72 (1981).
12. J. W. Nibler and G. V. Knighten, "Coherent anti-Stokes Raman spectroscopy," in *Raman Spectroscopy of Gases and Liquids*, A. Weber, ed. (Springer-Verlag, Berlin, 1979), pp. 253–299.
13. R. J. Hall and A. C. Eckbreth, "Coherent anti-Stokes Raman spectroscopy (CARS): Application to combustion di-

- agnostics," in *Laser Applications*, J. F. Ready and R. K. Erf, eds. (Academic, Orlando, Fla., 1984), Vol. 5, pp. 213–309.
14. R. L. Farrow, R. P. Lucht, G. L. Clark, and R. E. Palmer, "Species concentration measurements using CARS with nonresonant susceptibility normalization," *Appl. Opt.* **24**, 2241–2251 (1985).
 15. R. L. Farrow and L. A. Rahn, "Interpreting coherent anti-Stokes Raman spectra measured with multimode Nd:YAG pump lasers," *J. Opt. Soc. Am. B* **2**, 903–907 (1985).
 16. M. Alden and W. Wendt, "Application of CARS spectroscopy to the detection of SO₂," *Appl. Spectrosc.* **42**, 1421–1426 (1988).
 17. J. W. Hahn, S. N. Park, E. S. Lee, C. Rhee, K. T. Kang, S. H. Chung, C. Y. Choi, and Y. D. Huh, "Measuring the concentration of minor species from the modulation dip of the nonresonant background of broadband CARS spectra," *Appl. Spectrosc.* **47**, 710–714 (1993).
 18. J. Chang, J. Ducuing, and N. Bloembergen, "Relative phase measurement between fundamental and second-harmonic light," *Phys. Rev. Lett.* **15**, 6–8 (1965).
 19. Y. Yacoby, R. Fitzgibbon, and B. Lax, "Coherent cancellation of background in four-wave mixing spectroscopy," *J. Appl. Phys.* **51**, 3072–3077 (1980).
 20. G. Marowsky and G. Lupke, "CARS-background suppression by phase-controlled nonlinear interferometry," *Appl. Phys. B* **51**, 49–51 (1990).
 21. W. G. Rado, "The nonlinear third-order dielectric susceptibility coefficients of gases and optical third-harmonic generation," *Appl. Phys. Lett.* **11**, 123–125 (1967).
 22. T. Lundeen, S. Y. Hou, and J. W. Nibler, "Nonresonant third-order susceptibilities for various gases," *J. Chem. Phys.* **79**, 6301–6305 (1983).
 23. G. J. Rosasco and W. S. Hurst, "Measurement of resonant and nonresonant third-order nonlinear susceptibilities by coherent Raman spectroscopy," *Phys. Rev. A* **32**, 281–299 (1985).
 24. S. La and L. E. Harris, "Relative value of the third-order nonresonant susceptibility of water," *Appl. Opt.* **25**, 4501–4503 (1986).
 25. R. L. Farrow, R. P. Lucht, and L. A. Rahn, "Measurements of the nonresonant third-order susceptibilities of gases using coherent anti-Stokes Raman spectroscopy," *J. Opt. Soc. Am. B* **4**, 1241–1246 (1987).
 26. J. F. Ward and C. K. Miller, "Measurements of nonlinear optical polarizabilities for twelve small molecules," *Phys. Rev. A* **19**, 826–833 (1979).
 27. D. Heiman, R. W. Hellwarth, M. D. Levenson, and G. Martin, "Raman-induced Kerr effect," *Phys. Rev. Lett.* **36**, 189–192 (1976).
 28. G. J. Rosasco and W. S. Hurst, "Dispersion of the electronic contribution to the third-order nonlinear susceptibility of H₂," *J. Opt. Soc. Am. B* **3**, 1251–1256 (1986).
 29. E. S. Lee, J. W. Hahn, S. N. Park, and C. Rhee, "Study on the interference of nonlinear-optical signals," *J. Korean Opt. Soc.* **3**, 239–243 (1992).
 30. M. Born and E. Wolf, *Principle of Optics*, 5th ed. (Pergamon, Oxford, 1975), pp. 87–90.
 31. J. W. Hahn, S. N. Park, E. S. Lee, and C. Rhee, "Construction and performance test of a coherent anti-Stokes Raman spectrometer," *Korean J. Appl. Phys.* **4**, 314–320 (1991).
 32. A. C. Eckbreth, "BOXCARS: Cross-beam phase-matched CARS generation in gases," *Appl. Phys. Lett.* **32**, 421–423 (1978).
 33. J. W. Hahn, S. N. Park, and C. Rhee, "Fabry–Perot wavemeter for shot-by-shot analysis of pulsed lasers," *Appl. Opt.* **32**, 1095–1099 (1993).
 34. H. W. Schrotter and H. W. Klockner, "Raman scattering cross sections in gases and liquids," in *Raman Spectroscopy of Gases and Liquids*, A. Weber, ed. (Springer-Verlag, Berlin, 1979), pp. 123–166.
 35. J. Martin, "Raman intensities of propane in the gas phase," *J. Raman Spectrosc.* **16**, 139–142 (1985).
 36. M. G. Littman and H. J. Metcalf, "Spectral narrow pulsed dye laser without beam expander," *Appl. Opt.* **17**, 2224–2227 (1978).
 37. R. E. Palmer, "The CARSFIT computer code for calculating coherent anti-Stokes Raman spectra: user and programmer information," Sandia National Laboratories Rep. SAND89–8206.UC–13, 20 (Sandia National Laboratories, Livermore, Calif., 1989).
 38. G. Herzberg, *Molecular Spectra and Molecular Structure, II. Infrared and Raman Spectra of Polyatomic Molecules* (Van Nostrand Reinhold, New York, 1945), p. 276, pp. 370–372, pp. 394–395.
 39. W. L. Barnes, J. Susskind, R. H. Hunt, and E. K. Plyler, "Measurement and analysis of the ν_3 band of methane," *J. Chem. Phys.* **56**, 5160–5172 (1972).
 40. S. N. Suchard and J. E. Melzer, *Spectroscopic Data* (Information for Industry/Plenum, New York, 1976), Vol. 2, pp. 435–462.
 41. K. H. Hellwege, *Landolt–Bornstein Numerical Data and Functional Relationships in Science and Technology, Group II: Atomic and Molecular Physics* (Springer-Verlag, Berlin, 1983), Vol. 14, pp. 2–148.
 42. D. P. Shelton and J. E. Rice, "Measurements and calculations of the hyperpolarizabilities of atoms and small molecules in the gas phase," *Chem. Rev.* **94**, 3–29 (1994).
 43. B. Lange and J. Wolfrum, "The impact of laser field statistics in determination of temperature and concentration by multiple USED CARS," *Appl. Phys. B* **51**, 53–58 (1990).